Electronic correlations and evolution of the charge density wave in the kagome metals AV_3Sb_5 (A = K, Rb, Cs)

Xiaoxiang Zhou,[1,*] Yongkai Li,[2,3,*] Xinwei Fan,[1,*] Jiahao Hao,[1] Ying Xiang,[1] Zhe Liu,[1] Yaomin Dai,[1,†] Zhiwei Wang,[2,3,‡] Yugui Yao,[2,3] and Hai-Hu Wen[1,§]

[1]*National Laboratory of Solid State Microstructures and Department of Physics, Collaborative Innovation Center of Advanced Microstructures, Nanjing University, Nanjing 210093, China*

[2]*Key Laboratory of Advanced Optoelectronic Quantum Architecture and Measurement, Ministry of Education, School of Physics, Beijing Institute of Technology, Beijing 100081, China*

[3]*Micronano Center, Beijing Key Lab of Nanophotonics and Ultrafine Optoelectronic Systems, Beijing Institute of Technology, Beijing 100081, China*

(Received 26 July 2022; accepted 30 March 2023; published 12 April 2023)

The kagome metals AV_3Sb_5 (A = K, Rb, Cs) have attracted enormous interest as they exhibit an intertwined charge density wave (CDW) and superconductivity (SC). We report optical studies of AV_3Sb_5 across the whole family. With increasing alkali-metal atom radius from K to Cs, the CDW gap Δ_{CDW} increases monotonically, whereas T_{CDW} first rises and then drops, failing to establish a scaling relation with Δ_{CDW}. While the Fermi surface gapped by the CDW grows, T_c is elevated in CsV_3Sb_5, indicating that the interplay between the CDW and SC is not simply a competition for the density of states near E_F. More importantly, we observe an enhancement of electronic correlations in CsV_3Sb_5, which suppresses the CDW but enhances SC, accounting for all the above peculiar observations. Our results suggest electronic correlations as an important factor in manipulating the CDW and its entanglement with SC in AV_3Sb_5.

DOI: 10.1103/PhysRevB.107.165123

I. INTRODUCTION

The kagome lattice, composed of hexagons and corner-sharing triangles, provides a fascinating playground for exploring exotic quantum phenomena. For instance, spins or magnetic moments on a kagome lattice are subject to a high degree of geometric frustration that may lead to quantum spin liquids [1,2]; electrons in a kagome lattice form flat bands, Dirac points, and saddle points, which support intriguing quantum phenomena associated with nontrivial band topology [3–7] and a wide variety of electronic instabilities [8–11]. Particularly at van Hove filling, as a function of the on-site repulsion U and nearest-neighbor Coulomb interaction V, the kagome lattice exhibits a rich phase diagram consisting of various phases such as charge or spin bond order [10,11], superconductivity (SC) [8,10,11], charge density waves (CDWs) [11,12] and spin density waves (SDWs) [8].

The recently discovered kagome metals AV_3Sb_5 (A = K, Rb, Cs) [13] with the Fermi level E_F lying near the saddle points (van Hove filling) provide an excellent platform to realize the above exotic quantum states in real materials. Multiple topologically protected Dirac bands [14,15] and SC with a T_c of 0.92–2.5 K [14–16] have been reported in these compounds. In addition, a CDW transition occurs at T_{CDW} = 78, 103, and 94 K for KV_3Sb_5, RbV_3Sb_5, and CsV_3Sb_5, respectively [13–16]. Although a three-dimensional $2 \times 2 \times 2$ superlattice was observed in the CDW state [17,18], subsequent experimental results suggested a $2 \times 2 \times 4$ reconstruction [19] and even a transition between these two [20]. Upon entering the CDW state, a giant anomalous Hall effect [21,22] and electronic nematicity [23–27] also emerge. The application of pressure [28–31], uniaxial strain [32], or chemical doping [33–36] suppresses CDW, but enhances SC, signifying the competition between these two orders. While a variety of studies suggest that the saddle point or Fermi surface (FS) nesting plays an important role in driving the CDW instability [37–47], there is also evidence that the CDW is mainly driven by electron-phonon (e-ph) coupling [48–51]. At the present time, the driving mechanism of the CDW and how it interacts with SC in AV_3Sb_5 are subjects for intensive debate.

The evolution of the CDW and SC properties with alkali metal in AV_3Sb_5 may reveal key information about the interplay between the two orders. Here, we study the optical properties of AV_3Sb_5 across the whole family. As the alkali-metal atom radius grows from K to Cs, the CDW gap Δ_{CDW} increases monotonically, whereas T_{CDW} first rises but then drops, failing to exhibit a scaling relation with Δ_{CDW}. While the FS removed by Δ_{CDW} increases, T_c is raised in CsV_3Sb_5, indicating that the interplay between the CDW and SC is not simply a competition for the density of states (DOS) near E_F. Moreover, we observe an enhancement of electronic correlations in CsV_3Sb_5, which suppresses the CDW but promotes unconventional SC, accounting for the above peculiar behavior. Our results underline the importance of electronic correlations in manipulating the CDW and its entanglement with SC in AV_3Sb_5.

*These authors contributed equally to this work.
†ymdai@nju.edu.cn
‡zhiweiwang@bit.edu.cn
§hhwen@nju.edu.cn

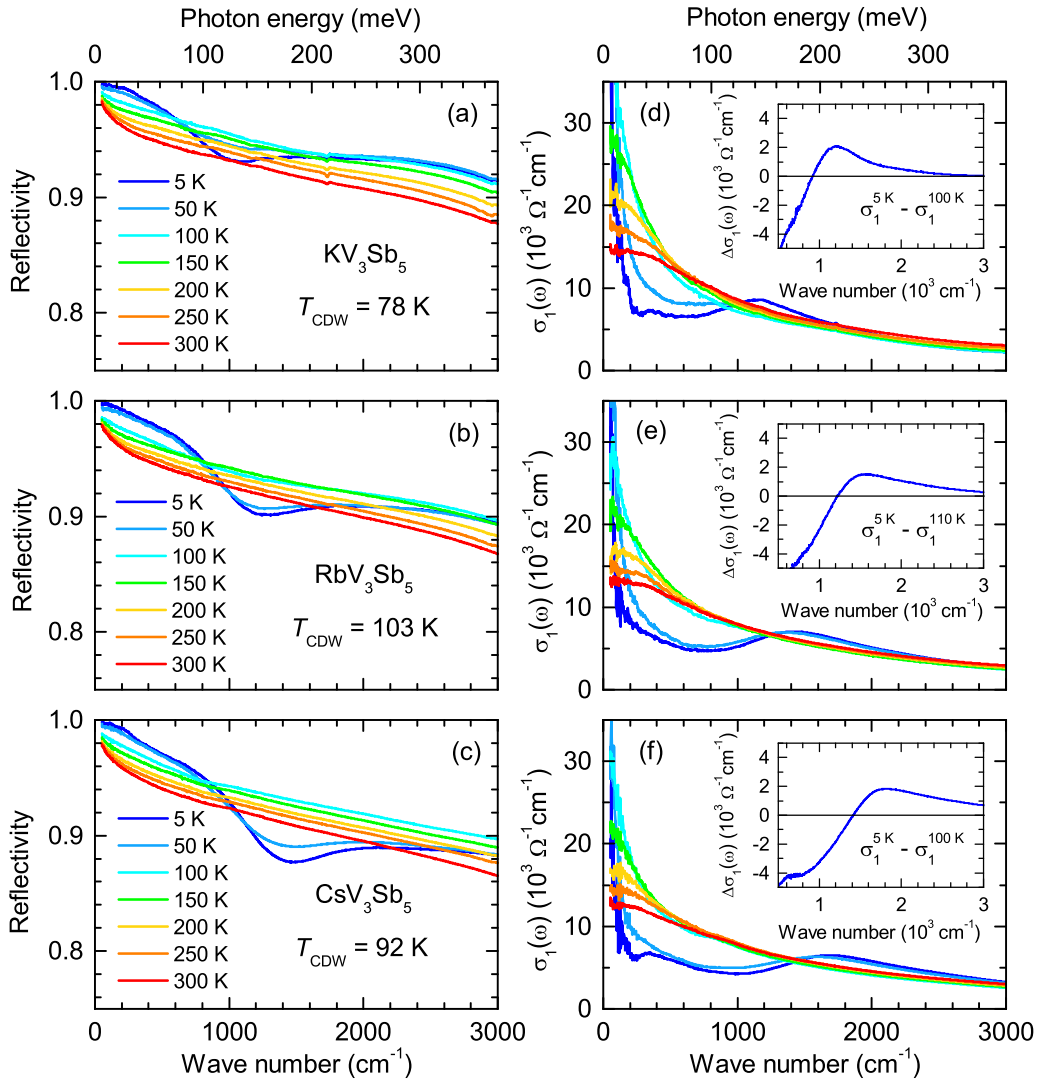

FIG. 1. (a)–(c) $R(\omega)$ at several representative temperatures for KV_3Sb_5, RbV_3Sb_5, and CsV_3Sb_5, respectively. (d)–(f) $\sigma_1(\omega)$ for KV_3Sb_5, RbV_3Sb_5, and CsV_3Sb_5, respectively. The inset displays $\Delta\sigma_1(\omega)$ at 5 K for each compound, where $\sigma_1(\omega)$ at T just above T_{CDW} is used as the base curve.

II. RESULTS AND DISCUSSION

The sample growth, characterization, and details of optical measurements are given in the Supplemental Material [52] (see, also, Refs. [53–56]). Figures 1(a)–1(c) show the reflectivity $R(\omega)$ at different temperatures for KV_3Sb_5, RbV_3Sb_5, and CsV_3Sb_5, respectively. Above T_{CDW}, $R(\omega)$ for all compounds exhibits metallic behavior: a very high $R(\omega)$ in the far-infrared range that approaches unity in the zero-frequency limit. Below T_{CDW}, a suppression of $R(\omega)$ around 1200 cm^{-1} occurs for all materials, signaling the opening of a CDW gap. As the alkali-metal atom radius grows from K to Cs, the suppression in $R(\omega)$ shifts to higher frequency and deepens, suggesting that the CDW gap increases in energy and the gap-induced FS modification intensifies with growing alkali-metal atom radius. The real part of the optical conductivity $\sigma_1(\omega)$ is obtained through a Kramers-Kronig analysis of $R(\omega)$ [52,57]. Figures 1(d)–1(f) show $\sigma_1(\omega)$ at different temperatures for KV_3Sb_5, RbV_3Sb_5, and CsV_3Sb_5, respectively. For all compounds, above T_{CDW}, a Drude response, i.e., a peak centered at zero frequency, can be clearly observed in the low-frequency $\sigma_1(\omega)$, in good agreement with the metallic nature of these materials; below T_{CDW}, a dramatic suppression of the low-frequency $\sigma_1(\omega)$ sets in, and the removed spectral weight [the area under $\sigma_1(\omega)$] is transferred to higher frequencies, which is the prototypical response of the CDW gap in $\sigma_1(\omega)$. The detailed evolution of $\sigma_1(\omega)$ with T is traced out in the 2D temperature-frequency ($T-\omega$) maps in Figs. 2(a)–2(c) for all three materials. The horizontal dashed line in each panel denotes T_{CDW}. Below T_{CDW}, the opening of the CDW gap leads to the presence of a blue region in the low-frequency range [a suppression of the low-frequency $\sigma_1(\omega)$] and a shift of the green/cyan region to higher frequencies. A comparison of Figs. 2(a)–2(c) reveals that as the radius of the alkali-metal atom in AV_3Sb_5 increases, the low-frequency blue region moves to higher frequencies and grows in area. These observations indicate that not only does the CDW gap value increase; the removed spectral weight due to the opening of the CDW gap also grows with increasing alkali-metal atom radius.

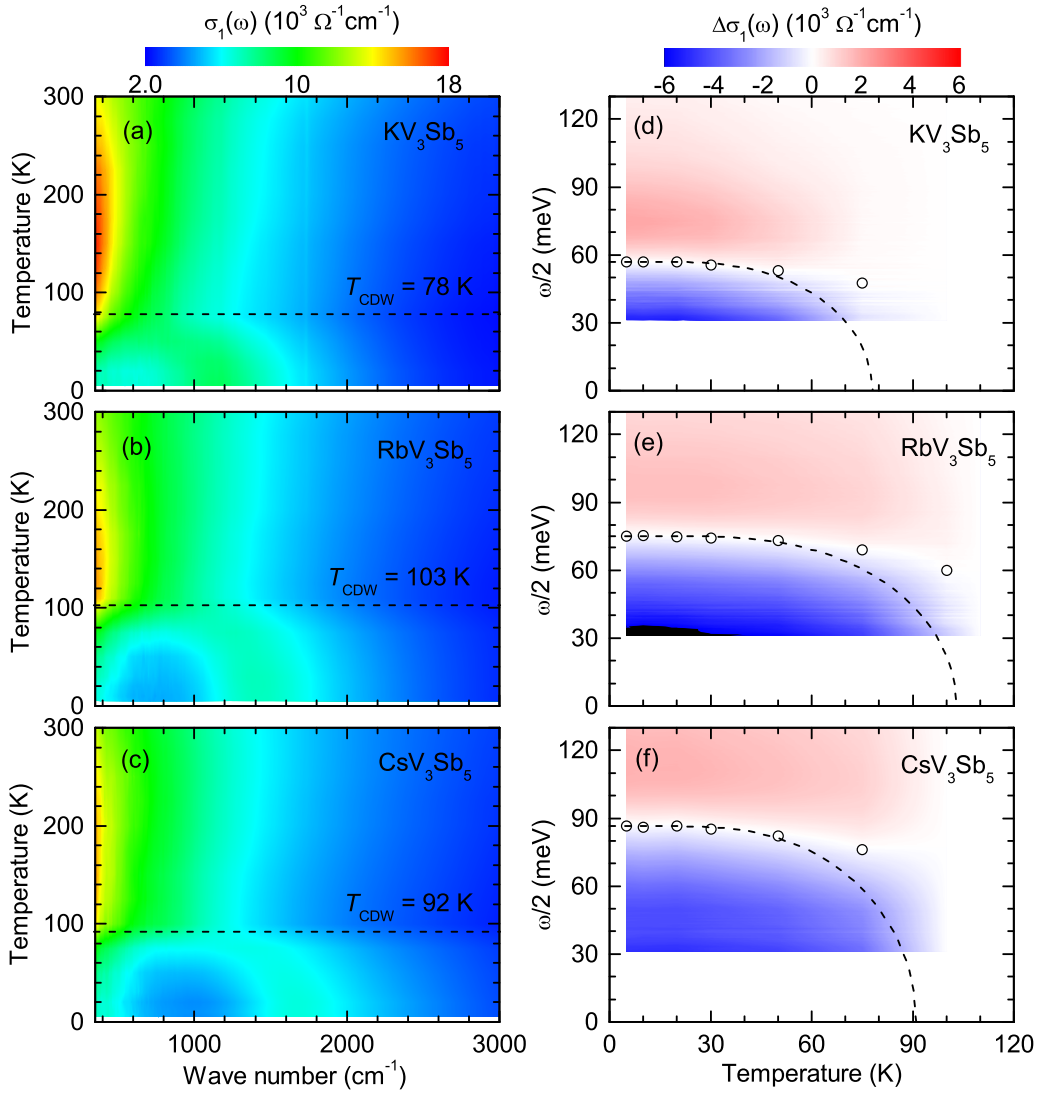

FIG. 2. (a)–(c) The 2D $T-\omega$ map of $\sigma_1(\omega)$ for KV_3Sb_5, RbV_3Sb_5, and CsV_3Sb_5, respectively. (d)–(f) $\Delta\sigma_1(\omega)$ in the 2D $\omega/2-T$ plot, where the white color (zero-crossing points) yields the T dependence of Δ_{CDW}. The dashed line in each panel represents the mean-field behavior.

The CDW gap Δ_{CDW} can be determined from the zero-crossing point in the difference optical conductivity,

$$\Delta\sigma_1(\omega) = \sigma_1^{T<T_{CDW}}(\omega) - \sigma_1^{P}(\omega), \tag{1}$$

where $\sigma_1^{T<T_{CDW}}(\omega)$ represents $\sigma_1(\omega)$ at $T < T_{CDW}$; $\sigma_1^{P}(\omega)$ refers to $\sigma_1(\omega)$ in the pristine phase. The insets of Figs. 1(d)–1(f) display $\Delta\sigma_1(\omega)$ at 5 K for KV_3Sb_5, RbV_3Sb_5, and CsV_3Sb_5, respectively, in which the zero-crossing point corresponds to $2\Delta_{CDW}$. Therefore, the T dependence of Δ_{CDW} can be obtained by plotting $\Delta\sigma_1(\omega)$ in the 2D $\omega/2-T$ map as shown in Figs. 2(d)–2(f) for KV_3Sb_5, RbV_3Sb_5, and CsV_3Sb_5, respectively, where the white color yields the evolution of Δ_{CDW} with T. For all materials, the T dependence of Δ_{CDW} deviates from the BCS mean-field behavior (dashed line) in the proximity of T_{CDW}, consistent with previous studies [39,58,59]. Moreover, Δ_{CDW} increases monotonically with increasing alkali-metal atom radius, failing to show a scaling relation with T_{CDW} which increases in RbV_3Sb_5 but then drops in CsV_3Sb_5. The values of Δ_{CDW} and T_{CDW} for AV_3Sb_5 are summarized in Figs. 4(a) and 4(b), respectively, for further discussions. Note that Δ_{CDW} can also be determined by alternative methods such as the extrapolation of the absorption edge in $\sigma_1(\omega)$ [58] and the position of the absorption peak [59]. We also extracted Δ_{CDW} using these methods [52] and found that different methods give different absolute values of Δ_{CDW}, but all methods yield consistent results. In previous work [39,58–60], Δ_{CDW} in different materials was determined by different methods, prohibiting an alkali-metal dependence study.

The removed spectral weight ΔS in the low-frequency range due to the opening of Δ_{CDW} reflects the gapped portion of the FS or the reduction of the DOS near E_F. ΔS can be directly obtained from the integral of $\sigma_1(\omega)$,

$$\Delta S = \int_0^{2\Delta_{CDW}} \left[\sigma_1^{P}(\omega) - \sigma_1^{T<T_{CDW}}(\omega)\right] d\omega. \tag{2}$$

The values of ΔS at $T = 5\,\mathrm{K}$ are 6.00, 6.49, and $6.74 \times 10^6\ \Omega^{-1}\,\mathrm{cm}^{-2}$ for KV_3Sb_5, RbV_3Sb_5, and CsV_3Sb_5,

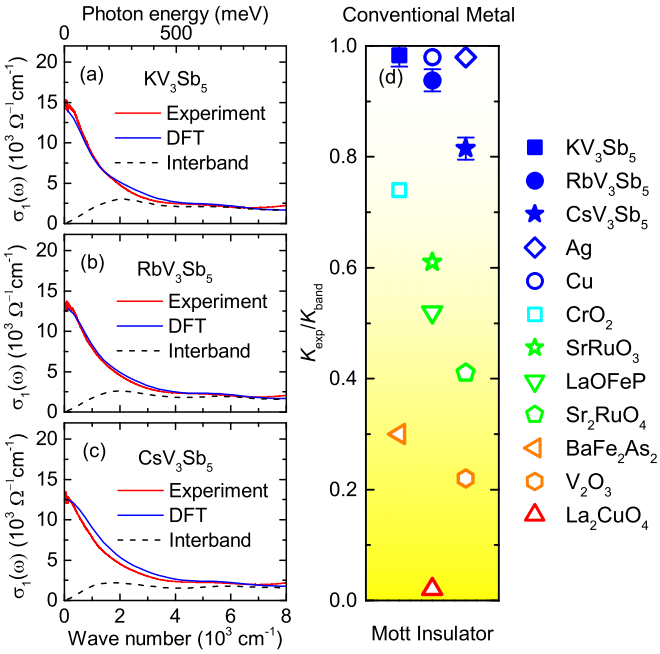

FIG. 3. (a)–(c) The calculated $\sigma_1(\omega)$ (blue solid curve) and the measured $\sigma_1(\omega)$ at 300 K (red solid curve) for KV_3Sb_5, RbV_3Sb_5, and CsV_3Sb_5, respectively. (d) K_{exp}/K_{band} for AV_3Sb_5 (solid symbols) and other representative materials (open symbols). The values of K_{exp}/K_{band} for other materials are obtained from Ref. [61] and the references cited therein.

respectively. The increase of ΔS with increasing alkali-metal atom radius indicates that a larger portion of the FS is removed by Δ_{CDW} in AV_3Sb_5 with a larger alkali-metal atom. We plot ΔS as a function of alkali metal in Fig. 4(d) for further discussions.

The ratio of the experimental kinetic energy K_{exp} to that from band theory K_{band} provides crucial information about electronic correlations [61–66]. The electron's kinetic energy for AV_3Sb_5 can be conveniently derived from the area under the Drude feature in $\sigma_1(\omega)$ [61,62],

$$K = \frac{2\hbar^2 c_0}{\pi e^2} \int_0^{\omega_c} \sigma_1(\omega) d\omega, \tag{3}$$

where c_0 is the distance between the V kagome layers, and ω_c is a cutoff frequency covering the entire Drude component in $\sigma_1(\omega)$. In order to determine K_{band}, we calculated the *ab*-plane $\sigma_1(\omega)$ for all three materials [52] (see, also, Refs. [67–70] therein). As depicted in Figs. 3(a)–3(c), the calculated $\sigma_1(\omega)$ spectra (blue curves) qualitatively agree with the measured ones (red curves). Due to the existence of low-energy interband transitions [52,58–60], the contributions from intraband and interband are not well separated in $\sigma_1(\omega)$. For an accurate determination of K_{exp}/K_{band}, we calculated the interband contribution in $\sigma_1(\omega)$ [black dashed lines in Figs. 3(a)–3(c)] and subtracted it from both the calculated and measured $\sigma_1(\omega)$. Using $\omega_c = 5000$ cm^{-1} for both K_{exp} and K_{band}, the values of K_{exp}/K_{band} are obtained for all three compounds.

Figure 3(d) summarizes K_{exp}/K_{band} for AV_3Sb_5 (solid symbols) and some other representative materials (open symbols). While conventional metals (Ag and Cu) have K_{exp}/K_{band} close to unity, K_{exp}/K_{band} for the well-known Mott insulators, such as La_2CuO_4, is almost zero due to on-site Coulomb repulsion which impedes the motion of electrons. Iron pnictides, e.g., LaOFeP and $BaFe_2As_2$, are categorized as moderately correlated materials, as their K_{exp}/K_{band} lie between conventional metals and Mott insulators. K_{exp}/K_{band} for AV_3Sb_5 fall into the range of 0.81–0.98, indicating weak electronic correlations. However, it is worth noting that while K_{exp}/K_{band} for KV_3Sb_5 and RbV_3Sb_5 are close to that of conventional metals, CsV_3Sb_5 features a reduced K_{exp}/K_{band}. Such a reduction of K_{exp}/K_{band} is not caused by a change of disorder or stoichiometry [52], but signifies an enhancement of electronic correlations. Theoretical calculations have revealed that the FS of AV_3Sb_5 is formed by Sb-5*p* and V-3*d* orbitals [37,71,72]. Since 3*d* electrons are subject to strong electronic correlations [73,74], the electronic correlations in AV_3Sb_5 are likely to arise from the V-3*d* orbitals. Recent ARPES studies have also found clear signatures of electronic correlations in the V-3*d* orbitals of CsV_3Sb_5 [46,75]. The enhancement of electronic correlations in CsV_3Sb_5 may originate from the extension of the V-V bond, as the V-V bond in CsV_3Sb_5 (2.7475 Å) is the longest [13]. However, the V-V bond in RbV_3Sb_5 (2.7358 Å) is shorter than that in KV_3Sb_5 (2.7409 Å), at odds with the slight decrease of K_{exp}/K_{band} in RbV_3Sb_5. Here, we would like to remark that the electronic correlations in AV_3Sb_5 are affected by multiple factors including the V-V bond length, the hybridization between V-3*d* and Sb-5*p* orbitals [71,76], and the filling of V-3*d* orbitals. The question of what factor plays a dominant role in tuning the electronic correlations calls for further studies. Given that the ground state of the kagome lattice sensitively depends on electronic correlations [10–12,38], the enhancement of electronic correlations in CsV_3Sb_5, although not as strong as that in cuprates and iron pnictides, may have an important influence on the CDW and its interplay with SC.

Essential information about the CDW and how it intertwines with SC in AV_3Sb_5 can be obtained from the alkali-metal dependence of the parameters summarized in Figs. 4(a)–4(f). A noticeable yet puzzling observation is that while Δ_{CDW} [Fig. 4(a)] increases monotonically with increasing alkali-metal atom radius, T_{CDW} [Fig. 4(b)] first increases but then decreases, failing to establish a scaling relation with Δ_{CDW}. This anomalous behavior is clearly at variance with the conventional CDW [77]. For both the nesting and e-ph coupling driven scenarios, a larger Δ_{CDW} would naturally support a higher T_{CDW}. Here in CsV_3Sb_5, an increase of Δ_{CDW} coincides with a decrease of T_{CDW}, implying that besides e-ph coupling and FS nesting, a competing factor that suppresses T_{CDW} also exerts considerable influence on the CDW. Furthermore, Fig. 4(c) shows that KV_3Sb_5 and RbV_3Sb_5 have the same $2\Delta_{CDW}/k_BT_{CDW}$, indicating that the CDW is governed by the same mechanism, whereas $2\Delta_{CDW}/k_BT_{CDW}$ is significantly larger in CsV_3Sb_5, suggesting that an extra factor is acting on the CDW order. Previous studies on transition metal dichalcogenides (TMDs) have documented that while e-ph coupling, FS nesting, and a high DOS are beneficial to the formation of CDW order, electronic correlations act as a competing factor which tends to localize the carriers and prevents the formation of CDW order [78,79]. Our optical

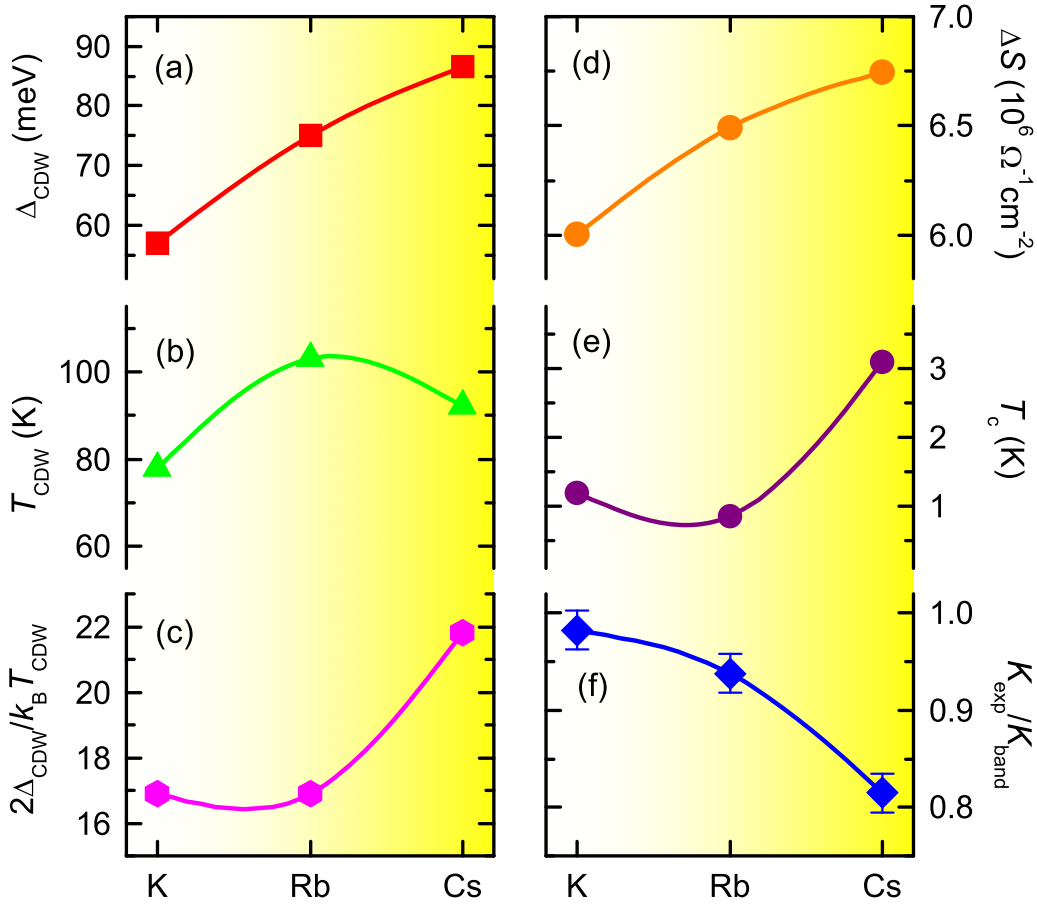

FIG. 4. The evolution of (a) Δ_{CDW}, (b) T_{CDW}, (c) $2\Delta_{CDW}/k_BT_{CDW}$, (d) ΔS, (e) T_c, and (f) K_{exp}/K_{band} with the alkali-metal atom in the AV_3Sb_5 family.

results have attested to the decrease of K_{exp}/K_{band} [Fig. 4(f)], i.e., the enhancement of electronic correlations in CsV_3Sb_5. These facts bring us to the possibility that the suppression of T_{CDW} and the larger $2\Delta_{CDW}/k_BT_{CDW}$ in CsV_3Sb_5 may be related to the enhancement of electronic correlations.

Other interesting observations emerge from the comparison of T_c, T_{CDW}, ΔS, and $2\Delta_{CDW}/k_BT_{CDW}$. As shown in Figs. 4(b) and 4(e), the suppression of T_{CDW} in CsV_3Sb_5 is accompanied by a rise of T_c, in accord with the competition between the CDW and SC reported by previous work [28–34]. Such a competition is not surprising, because the opening of the CDW gap depletes the DOS near E_F, resulting in a suppression of SC [80]. However, Figs. 4(d) and 4(e) reveal that the rise of T_c in CsV_3Sb_5 coincides with an increase of ΔS. This implies that the CDW and SC in AV_3Sb_5 do not share the same DOS, so that the competition between the CDW and SC is not simply through competing for effective DOS near E_F, but manipulated by other factors. It is noteworthy that $2\Delta_{CDW}/k_BT_{CDW}$ [Fig. 4(c)] and T_c [Fig. 4(e)] exhibit similar alkali-metal dependence, which may provide more insights. The larger $2\Delta_{CDW}/k_BT_{CDW}$ in CsV_3Sb_5 implies a shorter CDW correlation length [81]. Previous studies on TMDs [82–85] and cuprates [86] have revealed that disorder reduces the CDW correlation length, and raises T_c, which may be responsible for the similar trends in $2\Delta_{CDW}/k_BT_{CDW}$ and T_c. However, our CsV_3Sb_5 sample has the highest residual resistivity ratio [52], indicating the lowest disorder, which rules out the disorder scenario. Alternatively, the enhancement of electronic correlations diminishes the spatial extension of the electronic wave functions and tends to localize the carriers [79], which also leads to a shorter CDW correlation length, i.e., a larger $2\Delta_{CDW}/k_BT_{CDW}$; a recent theoretical study has shown that electronic correlations suppress the charge susceptibility but enhance spin fluctuations [78], which are believed to mediate unconventional SC [87]; furthermore, extensive studies on cuprates and iron pnictides have underlined the importance of electronic correlations in generating unconventional SC [74,88]. Combining these facts with our observations, we argue that electronic correlations may be a key parameter controlling the evolution of $2\Delta_{CDW}/k_BT_{CDW}$ and T_c, as well as the competition between CDW and SC in AV_3Sb_5.

III. CONCLUSIONS

To summarize, we performed a systematic investigation into the optical properties of AV_3Sb_5 across the whole family. We found that as the alkali-metal atom radius grows from K to Cs, (i) while Δ_{CDW} increases monotonically, T_{CDW} rises in RbV_3Sb_5 but then drops in CsV_3Sb_5, at odds with conventional CDW; (ii) the FS removed by Δ_{CDW} increases, whereas T_c is enhanced in CsV_3Sb_5, suggesting that the interplay between the CDW and SC is not simply a competition for effective DOS near E_F; (iii) K_{exp}/K_{band} is reduced, indicat-

ing an enhancement of electronic correlations. An analysis considering all the above observations and previous work suggests that the enhancement of electronic correlations may be a decisive factor that controls the formation of the CDW order and its entanglement with SC in AV_3Sb_5.

Note added. A recent optical study reported stronger electronic correlations in KV_3Sb_5 and RbV_3Sb_5 [60]. The low-frequency $\sigma_1(\omega)$ of their KV_3Sb_5 [59] and RbV_3Sb_5 [60] are dominated by multiple absorption peaks arising from interband transitions and IR-active phonons, in contrast to our $\sigma_1(\omega)$ which only exhibit a pronounced Drude response. In Refs. [58–60], to find a good agreement between experiment and calculations, E_F is shifted upwards by 64 meV for KV_3Sb_5 and by 41 meV for RbV_3Sb_5; such an E_F shift is not required for CsV_3Sb_5. The upward shift of E_F significantly enhances low-energy interband transitions [58–60]. This implies that the discrepancies in the findings may stem from a difference in E_F of the sample. In this context, the question of how E_F affects electronic correlations in AV_3Sb_5 is of great interest, which deserves further investigations.

ACKNOWLEDGMENTS

We thank Hu Miao, R. Thomale, Qianghua Wang, Nanlin Wang, Xiaoxiang Xi, Bing Xu, Binghai Yan, Huan Yang, Run Yang, Shunli Yu, Peng Zhang, and Jianzhou Zhao for helpful discussions. We gratefully acknowledge financial support from the National Key R&D Program of China (Grants No. 2016YFA0300401 and No. 2020YFA0308800), the National Natural Science Foundation of China (Grants No. 12174180, No. 11874206, No. 12061131001, No. 92065109, No. 11734003, and No. 11904294), the Fundamental Research Funds for the Central Universities (Grant No. 020414380095), the Jiangsu Shuangchuang program, the Beijing Natural Science Foundation (Grants No. Z190006 and No. Z210006), and the Beijing Institute of Technology Research Fund Program for Young Scholars (Grant No. 3180012222011).

[1] L. Balents, Spin liquids in frustrated magnets, Nature (London) **464**, 199 (2010).

[2] S. Yan, D. A. Huse, and S. R. White, Spin-liquid ground state of the $S = 1/2$ kagome Heisenberg antiferromagnet, Science **332**, 1173 (2011).

[3] I. I. Mazin, H. O. Jeschke, F. Lechermann, H. Lee, M. Fink, R. Thomale, and R. Valentí, Theoretical prediction of a strongly correlated Dirac metal, Nat. Commun. **5**, 4261 (2014).

[4] L. Ye, M. Kang, J. Liu, F. von Cube, C. R. Wicker, T. Suzuki, C. Jozwiak, A. Bostwick, E. Rotenberg, D. C. Bell, L. Fu, R. Comin, and J. G. Checkelsky, Massive Dirac fermions in a ferromagnetic kagome metal, Nature (London) **555**, 638 (2018).

[5] M. Kang, L. Ye, S. Fang, J.-S. You, A. Levitan, M. Han, J. I. Facio, C. Jozwiak, A. Bostwick, E. Rotenberg, M. K. Chan, R. D. McDonald, D. Graf, K. Kaznatcheev, E. Vescovo, D. C. Bell, E. Kaxiras, J. van den Brink, M. Richter, M. Prasad Ghimire *et al.*, Dirac fermions and flat bands in the ideal kagome metal FeSn, Nat. Mater. **19**, 163 (2020).

[6] M. Kang, S. Fang, L. Ye, H. C. Po, J. Denlinger, C. Jozwiak, A. Bostwick, E. Rotenberg, E. Kaxiras, J. G. Checkelsky, and R. Comin, Topological flat bands in frustrated kagome lattice CoSn, Nat. Commun. **11**, 4004 (2020).

[7] Z. Liu, M. Li, Q. Wang, G. Wang, C. Wen, K. Jiang, X. Lu, S. Yan, Y. Huang, D. Shen, J.-X. Yin, Z. Wang, Z. Yin, H. Lei, and S. Wang, Orbital-selective Dirac fermions and extremely flat bands in frustrated kagome-lattice metal CoSn, Nat. Commun. **11**, 4002 (2020).

[8] S.-L. Yu and J.-X. Li, Chiral superconducting phase and chiral spin-density-wave phase in a Hubbard model on the kagome lattice, Phys. Rev. B **85**, 144402 (2012).

[9] M. L. Kiesel and R. Thomale, Sublattice interference in the kagome Hubbard model, Phys. Rev. B **86**, 121105(R) (2012).

[10] M. L. Kiesel, C. Platt, and R. Thomale, Unconventional Fermi Surface Instabilities in the Kagome Hubbard Model, Phys. Rev. Lett. **110**, 126405 (2013).

[11] W.-S. Wang, Z.-Z. Li, Y.-Y. Xiang, and Q.-H. Wang, Competing electronic orders on kagome lattices at van Hove filling, Phys. Rev. B **87**, 115135 (2013).

[12] F. Ferrari, F. Becca, and R. Valentí, Charge density waves in kagome-lattice extended Hubbard models at the van Hove filling, Phys. Rev. B **106**, L081107 (2022).

[13] B. R. Ortiz, L. C. Gomes, J. R. Morey, M. Winiarski, M. Bordelon, J. S. Mangum, I. W. H. Oswald, J. A. Rodriguez-Rivera, J. R. Neilson, S. D. Wilson, E. Ertekin, T. M. McQueen, and E. S. Toberer, New kagome prototype materials: Discovery of KV_3Sb_5, RbV_3Sb_5, and CsV_3Sb_5, Phys. Rev. Mater. **3**, 094407 (2019).

[14] B. R. Ortiz, S. M. L. Teicher, Y. Hu, J. L. Zuo, P. M. Sarte, E. C. Schueller, A. M. Milinda Abeykoon, M. J. Krogstad, S. Rosenkranz, R. Osborn, R. Seshadri, L. Balents, J. He, and S. D. Wilson, CsV_3Sb_5: A $\mathbb{Z}_2$ Topological Kagome Metal with a Superconducting Ground State, Phys. Rev. Lett. **125**, 247002 (2020).

[15] Q. Yin, Z. Tu, C. Gong, Y. Fu, S. Yan, and H. Lei, Superconductivity and normal-state properties of kagome metal RbV_3Sb_5 single crystals, Chin. Phys. Lett. **38**, 037403 (2021).

[16] B. R. Ortiz, P. M. Sarte, E. M. Kenney, M. J. Graf, S. M. L. Teicher, R. Seshadri, and S. D. Wilson, Superconductivity in the $\mathbb{Z}_2$ kagome metal KV_3Sb_5, Phys. Rev. Mater. **5**, 034801 (2021).

[17] Z. Liang, X. Hou, F. Zhang, W. Ma, P. Wu, Z. Zhang, F. Yu, J.-J. Ying, K. Jiang, L. Shan, Z. Wang, and X.-H. Chen, Three-Dimensional Charge Density Wave and Surface-Dependent Vortex-Core States in a Kagome Superconductor CsV_3Sb_5, Phys. Rev. X **11**, 031026 (2021).

[18] H. Li, T. T. Zhang, T. Yilmaz, Y. Y. Pai, C. E. Marvinney, A. Said, Q. W. Yin, C. S. Gong, Z. J. Tu, E. Vescovo, C. S. Nelson, R. G. Moore, S. Murakami, H. C. Lei, H. N. Lee, B. J. Lawrie, and H. Miao, Observation of Unconventional Charge Density Wave without Acoustic Phonon Anomaly in Kagome Superconductors AV_3Sb_5 (A = Rb, Cs), Phys. Rev. X **11**, 031050 (2021).

[19] B. R. Ortiz, S. M. L. Teicher, L. Kautzsch, P. M. Sarte, N. Ratcliff, J. Harter, J. P. C. Ruff, R. Seshadri, and S. D. Wilson, Fermi Surface Mapping and the Nature of Charge-Density-Wave Order in the Kagome Superconductor CsV_3Sb_5, Phys. Rev. X **11**, 041030 (2021).

[20] Q. Stahl, D. Chen, T. Ritschel, C. Shekhar, E. Sadrollahi, M. C. Rahn, O. Ivashko, M. v. Zimmermann, C. Felser, and J. Geck, Temperature-driven reorganization of electronic order in CsV_3Sb_5, Phys. Rev. B **105**, 195136 (2022).

[21] S.-Y. Yang, Y. Wang, B. R. Ortiz, D. Liu, J. Gayles, E. Derunova, R. Gonzalez-Hernandez, L. Šmejkal, Y. Chen, S. S. P. Parkin, S. D. Wilson, E. S. Toberer, T. McQueen, and M. N. Ali, Giant, unconventional anomalous Hall effect in the metallic frustrated magnet candidate, KV_3Sb_5, Sci. Adv. **6**, eabb6003 (2020).

[22] F. H. Yu, T. Wu, Z. Y. Wang, B. Lei, W. Z. Zhuo, J. J. Ying, and X. H. Chen, Concurrence of anomalous Hall effect and charge density wave in a superconducting topological kagome metal, Phys. Rev. B **104**, L041103 (2021).

[23] Y. Xiang, Q. Li, Y. Li, W. Xie, H. Yang, Z. Wang, Y. Yao, and H.-H. Wen, Twofold symmetry of c-axis resistivity in topological kagome superconductor CsV_3Sb_5 with in-plane rotating magnetic field, Nat. Commun. **12**, 6727 (2021).

[24] H. Chen, H. Yang, B. Hu, Z. Zhao, J. Yuan, Y. Xing, G. Qian, Z. Huang, G. Li, Y. Ye, S. Ma, S. Ni, H. Zhang, Q. Yin, C. Gong, Z. Tu, H. Lei, H. Tan, S. Zhou, C. Shen *et al.*, Roton pair density wave in a strong-coupling kagome superconductor, Nature (London) **599**, 222 (2021).

[25] H. Li, H. Zhao, B. R. Ortiz, T. Park, M. Ye, L. Balents, Z. Wang, S. D. Wilson, and I. Zeljkovic, Rotation symmetry breaking in the normal state of a kagome superconductor KV_3Sb_5, Nat. Phys. **18**, 265 (2022).

[26] Q. Wu, Z. X. Wang, Q. M. Liu, R. S. Li, S. X. Xu, Q. W. Yin, C. S. Gong, Z. J. Tu, H. C. Lei, T. Dong, and N. L. Wang, Simultaneous formation of two-fold rotation symmetry with charge order in the kagome superconductor CsV_3Sb_5 by optical polarization rotation measurement, Phys. Rev. B **106**, 205109 (2022).

[27] Y. Xu, Z. Ni, Y. Liu, B. R. Ortiz, Q. Deng, S. D. Wilson, B. Yan, L. Balents, and L. Wu, Three-state nematicity and magneto-optical Kerr effect in the charge density waves in kagome superconductors, Nat. Phys. **18**, 1470 (2022).

[28] F. H. Yu, D. H. Ma, W. Z. Zhuo, S. Q. Liu, X. K. Wen, B. Lei, J. J. Ying, and X. H. Chen, Unusual competition of superconductivity and charge-density-wave state in a compressed topological kagome metal, Nat. Commun. **12**, 3645 (2021).

[29] K. Y. Chen, N. N. Wang, Q. W. Yin, Y. H. Gu, K. Jiang, Z. J. Tu, C. S. Gong, Y. Uwatoko, J. P. Sun, H. C. Lei, J. P. Hu, and J.-G. Cheng, Double Superconducting Dome and Triple Enhancement of T_c in the Kagome Superconductor CsV_3Sb_5 under High Pressure, Phys. Rev. Lett. **126**, 247001 (2021).

[30] F. Du, S. Luo, B. R. Ortiz, Y. Chen, W. Duan, D. Zhang, X. Lu, S. D. Wilson, Y. Song, and H. Yuan, Pressure-induced double superconducting domes and charge instability in the kagome metal KV_3Sb_5, Phys. Rev. B **103**, L220504 (2021).

[31] Z. Zhang, Z. Chen, Y. Zhou, Y. Yuan, S. Wang, J. Wang, H. Yang, C. An, L. Zhang, X. Zhu, Y. Zhou, X. Chen, J. Zhou, and Z. Yang, Pressure-induced reemergence of superconductivity in the topological kagome metal CsV_3Sb_5, Phys. Rev. B **103**, 224513 (2021).

[32] T. Qian, M. H. Christensen, C. Hu, A. Saha, B. M. Andersen, R. M. Fernandes, T. Birol, and N. Ni, Revealing the competition between charge density wave and superconductivity in CsV_3Sb_5 through uniaxial strain, Phys. Rev. B **104**, 144506 (2021).

[33] Y. Song, T. Ying, X. Chen, X. Han, X. Wu, A. P. Schnyder, Y. Huang, J.-g. Guo, and X. Chen, Competition of Superconductivity and Charge Density Wave in Selective Oxidized CsV_3Sb_5 Thin Flakes, Phys. Rev. Lett. **127**, 237001 (2021).

[34] Y. M. Oey, B. R. Ortiz, F. Kaboudvand, J. Frassineti, E. Garcia, R. Cong, S. Sanna, V. F. Mitrović, R. Seshadri, and S. D. Wilson, Fermi level tuning and double-dome superconductivity in the kagome metal $CsV_3Sb_{5-x}Sn_x$, Phys. Rev. Mater. **6**, L041801 (2022).

[35] Y. Li, Q. Li, X. Fan, J. Liu, Q. Feng, M. Liu, C. Wang, J.-X. Yin, J. Duan, X. Li, Z. Wang, H.-H. Wen, and Y. Yao, Tuning the competition between superconductivity and charge order in the kagome superconductor $Cs(V_{1-x}Nb_x)_3Sb_5$, Phys. Rev. B **105**, L180507 (2022).

[36] Y. Liu, Y. Wang, Y. Cai, Z. Hao, X.-M. Ma, L. Wang, C. Liu, J. Chen, L. Zhou, J. Wang, S. Wang, H. He, Y. Liu, S. Cui, J. Wang, B. Huang, C. Chen, and J.-W. Mei, Doping evolution of superconductivity, charge order and band topology in hole-doped topological kagome superconductors $Cs(V_{1-x}Ti_x)_3Sb_5$, arXiv:2110.12651.

[37] H. Tan, Y. Liu, Z. Wang, and B. Yan, Charge Density Waves and Electronic Properties of Superconducting Kagome Metals, Phys. Rev. Lett. **127**, 046401 (2021).

[38] M. M. Denner, R. Thomale, and T. Neupert, Analysis of Charge Order in the Kagome Metal AV_3Sb_5 ($A = \mathrm{K}, \mathrm{Rb}, \mathrm{Cs}$), Phys. Rev. Lett. **127**, 217601 (2021).

[39] X. Zhou, Y. Li, X. Fan, J. Hao, Y. Dai, Z. Wang, Y. Yao, and H.-H. Wen, Origin of charge density wave in the kagome metal CsV_3Sb_5 as revealed by optical spectroscopy, Phys. Rev. B **104**, L041101 (2021).

[40] M. H. Christensen, T. Birol, B. M. Andersen, and R. M. Fernandes, Theory of the charge density wave in AV_3Sb_5 kagome metals, Phys. Rev. B **104**, 214513 (2021).

[41] Z. Wang, S. Ma, Y. Zhang, H. Yang, Z. Zhao, Y. Ou, Y. Zhu, S. Ni, Z. Lu, H. Chen, K. Jiang, L. Yu, Y. Zhang, X. Dong, J. Hu, H.-J. Gao, and Z. Zhao, Distinctive momentum dependent charge-density-wave gap observed in CsV_3Sb_5 superconductor with topological kagome lattice, arXiv:2104.05556.

[42] S. Cho, H. Ma, W. Xia, Y. Yang, Z. Liu, Z. Huang, Z. Jiang, X. Lu, J. Liu, Z. Liu, J. Li, J. Wang, Y. Liu, J. Jia, Y. Guo, J. Liu, and D. Shen, Emergence of New van Hove Singularities in the Charge Density Wave State of a Topological Kagome Metal RbV_3Sb_5, Phys. Rev. Lett. **127**, 236401 (2021).

[43] R. Lou, A. Fedorov, Q. Yin, A. Kuibarov, Z. Tu, C. Gong, E. F. Schwier, B. Büchner, H. Lei, and S. Borisenko, Charge-Density-Wave-Induced Peak-Dip-Hump Structure and the Multiband Superconductivity in a Kagome Superconductor CsV_3Sb_5, Phys. Rev. Lett. **128**, 036402 (2022).

[44] T. M. Rice and G. K. Scott, New Mechanism for a Charge-Density-Wave Instability, Phys. Rev. Lett. **35**, 120 (1975).

[45] M. Kang, S. Fang, J.-K. Kim, B. R. Ortiz, S. H. Ryu, J. Kim, J. Yoo, G. Sangiovanni, D. Di Sante, B.-G. Park, C. Jozwiak, A. Bostwick, E. Rotenberg, E. Kaxiras, S. D. Wilson, J.-H.

Park, and R. Comin, Twofold van Hove singularity and origin of charge order in topological kagome superconductor CsV_3Sb_5, Nat. Phys. **18**, 301 (2022).

[46] Y. Hu, X. Wu, B. R. Ortiz, S. Ju, X. Han, J. Ma, N. C. Plumb, M. Radovic, R. Thomale, S. D. Wilson, A. P. Schnyder, and M. Shi, Rich nature of Van Hove singularities in Kagome superconductor CsV_3Sb_5, Nat. Commun. **13**, 2220 (2022).

[47] Z. Liu, N. Zhao, Q. Yin, C. Gong, Z. Tu, M. Li, W. Song, Z. Liu, D. Shen, Y. Huang, K. Liu, H. Lei, and S. Wang, Charge-Density-Wave-Induced Bands Renormalization and Energy Gaps in a Kagome Superconductor RbV_3Sb_5, Phys. Rev. X **11**, 041010 (2021).

[48] H. Luo, Q. Gao, H. Liu, Y. Gu, D. Wu, C. Yi, J. Jia, S. Wu, X. Luo, Y. Xu, L. Zhao, Q. Wang, H. Mao, G. Liu, Z. Zhu, Y. Shi, K. Jiang, J. Hu, Z. Xu, and X. J. Zhou, Electronic nature of charge density wave and electron-phonon coupling in kagome superconductor KV_3Sb_5, Nat. Commun. **13**, 273 (2022).

[49] Y. Xie, Y. Li, P. Bourges, A. Ivanov, Z. Ye, J.-X. Yin, M. Z. Hasan, A. Luo, Y. Yao, Z. Wang, G. Xu, and P. Dai, Electron-phonon coupling in the charge density wave state of CsV_3Sb_5, Phys. Rev. B **105**, L140501 (2022).

[50] J.-G. Si, W.-J. Lu, Y.-P. Sun, P.-F. Liu, and B.-T. Wang, Charge density wave and pressure-dependent superconductivity in the kagome metal CsV_3Sb_5: A first-principles study, Phys. Rev. B **105**, 024517 (2022).

[51] G. Liu, X. Ma, K. He, Q. Li, H. Tan, Y. Liu, J. Xu, W. Tang, K. Watanabe, T. Taniguchi, L. Gao, Y. Dai, H.-H. Wen, B. Yan, and X. Xi, Observation of anomalous amplitude modes in the kagome metal CsV_3Sb_5, Nat. Commun. **13**, 3461 (2022).

[52] See Supplemental Material at http://link.aps.org/supplemental/10.1103/PhysRevB.107.165123 for details about sample synthesis, sample characterizations, optical measurements, and first-principles calculations.

[53] Z. Wang, Y.-X. Jiang, J.-X. Yin, Y. Li, G.-Y. Wang, H.-L. Huang, S. Shao, J. Liu, P. Zhu, N. Shumiya, M. S. Hossain, H. Liu, Y. Shi, J. Duan, X. Li, G. Chang, P. Dai, Z. Ye, G. Xu, Y. Wang *et al.*, Electronic nature of chiral charge order in the kagome superconductor CsV_3Sb_5, Phys. Rev. B **104**, 075148 (2021).

[54] Z. Wang, K. Segawa, S. Sasaki, A. A.Taskin, and Y. Ando, Ferromagnetism in Cr-doped topological insulator $TlSbTe_2$, APL Mater. **3**, 083302 (2015).

[55] Z. Wang, A. A. Taskin, T. Frölich, M. Braden, and Y. Ando, Superconductivity in $Tl_{0.6}Bi_2Te_3$ derived from a topological insulator, Chem. Mater. **28**, 779 (2016).

[56] C. C. Homes, M. Reedyk, D. A. Cradles, and T. Timusk, Technique for measuring the reflectance of irregular, submillimeter-sized samples, Appl. Opt. **32**, 2976 (1993).

[57] M. Dressel and G. Grüner, *Electrodynamics of Solids* (Cambridge University Press, 2002).

[58] E. Uykur, B. R. Ortiz, O. Iakutkina, M. Wenzel, S. D. Wilson, M. Dressel, and A. A. Tsirlin, Low-energy optical properties of the nonmagnetic kagome metal CsV_3Sb_5, Phys. Rev. B **104**, 045130 (2021).

[59] E. Uykur, B. R. Ortiz, S. D. Wilson, M. Dressel, and A. A. Tsirlin, Optical detection of the density-wave instability in the kagome metal KV_3Sb_5, npj Quantum Mater. **7**, 16 (2022).

[60] M. Wenzel, B. R. Ortiz, S. D. Wilson, M. Dressel, A. A. Tsirlin, and E. Uykur, Optical study of RbV_3Sb_5: Multiple density-wave gaps and phonon anomalies, Phys. Rev. B **105**, 245123 (2022).

[61] M. M. Qazilbash, J. J. Hamlin, R. E. Baumbach, L. Zhang, D. J. Singh, M. B. Maple, and D. N. Basov, Electronic correlations in the iron pnictides, Nat. Phys. **5**, 647 (2009).

[62] A. J. Millis, A. Zimmers, R. P. S. M. Lobo, N. Bontemps, and C. C. Homes, Mott physics and the optical conductivity of electron-doped cuprates, Phys. Rev. B **72**, 224517 (2005).

[63] Y. Xu, J. Zhao, C. Yi, Q. Wang, Q. Yin, Y. Wang, X. Hu, L. Wang, E. Liu, G. Xu, L. Lu, A. A. Soluyanov, H. Lei, Y. Shi, J. Luo, and Z.-G. Chen, Electronic correlations and flattened band in magnetic Weyl semimetal candidate $Co_3Sn_2S_2$, Nat. Commun. **11**, 3985 (2020).

[64] L. Degiorgi, Electronic correlations in iron-pnictide superconductors and beyond: Lessons learned from optics, New J. Phys. **13**, 023011 (2011).

[65] Y. Shao, A. N. Rudenko, J. Hu, Z. Sun, Y. Zhu, S. Moon, A. J. Millis, S. Yuan, A. I. Lichtenstein, D. Smirnov, Z. Q. Mao, M. I. Katsnelson, and D. N. Basov, Electronic correlations in nodal-line semimetals, Nat. Phys. **16**, 636 (2020).

[66] M. Nakajima, T. Tanaka, S. Ishida, K. Kihou, C. H. Lee, A. Iyo, T. Kakeshita, H. Eisaki, and S. Uchida, Crossover from bad to good metal in $BaFe_2(As_{1-x}P_x)_2$ induced by isovalent P substitution, Phys. Rev. B **88**, 094501 (2013).

[67] P. Blaha, K. Schwarz, G. K. H. Madsen, D. Kvasnicka, and J. Luitz, *WIEN2k, An Augmented Plane Wave + Local Orbitals Program for Calculating Crystal Properties* (Technische Universität Wien, Vienna, Austria, 2001).

[68] K. Schwarz and P. Blaha, Solid state calculations using WIEN2k, Comput. Mater. Sci. **28**, 259 (2003).

[69] R. Abt, C. Ambrosch-Draxl, and P. Knoll, Optical response of high temperature superconductors by full potential LAPW band structure calculations, Phys. B: Condens. Matter **194-196**, 1451 (1994).

[70] C. Ambrosch-Draxl and J. O. Sofo, Linear optical properties of solids within the full-potential linearized augmented planewave method, Comput. Phys. Commun. **175**, 1 (2006).

[71] J. Zhao, W. Wu, Y. Wang, and S. A. Yang, Electronic correlations in the normal state of the kagome superconductor KV_3Sb_5, Phys. Rev. B **103**, L241117 (2021).

[72] H. LaBollita and A. S. Botana, Tuning the Van Hove singularities in AV_3Sb_5(A = K, Rb, Cs) via pressure and doping, Phys. Rev. B **104**, 205129 (2021).

[73] M. Imada, A. Fujimori, and Y. Tokura, Metal-insulator transitions, Rev. Mod. Phys. **70**, 1039 (1998).

[74] R. Yu, H. Hu, E. M. Nica, J.-X. Zhu, and Q. Si, Orbital selectivity in electron correlations and superconducting pairing of iron-based superconductors, Front. Phys. **9**, 578347 (2021).

[75] Y. Hu, S. M. Teicher, B. R. Ortiz, Y. Luo, S. Peng, L. Huai, J. Ma, N. C. Plumb, S. D. Wilson, J. He, and M. Shi, Topological surface states and flat bands in the kagome superconductor CsV_3Sb_5, Sci. Bull. **67**, 495 (2022).

[76] M. Y. Jeong, H.-J. Yang, H. S. Kim, Y. B. Kim, S. B. Lee, and M. J. Han, Crucial role of out-of-plane Sb p orbitals in Van Hove singularity formation and electronic correlations in

the superconducting kagome metal CsV_3Sb_5, Phys. Rev. B **105**, 235145 (2022).

[77] G. Grüner, The dynamics of charge-density waves, Rev. Mod. Phys. **60**, 1129 (1988).

[78] E. G. C. P. van Loon, M. Rösner, G. Schönhoff, M. I. Katsnelson, and T. O. Wehling, Competing Coulomb and electron-phonon interactions in NbS_2, npj Quantum Mater. **3**, 32 (2018).

[79] D. Lin, S. Li, J. Wen, H. Berger, L. Forró, H. Zhou, S. Jia, T. Taniguchi, K. Watanabe, X. Xi, and M. S. Bahramy, Patterns and driving forces of dimensionality-dependent charge density waves in $2H$-type transition metal dichalcogenides, Nat. Commun. **11**, 2406 (2020).

[80] G. Bilbro and W. L. McMillan, Theoretical model of superconductivity and the martensitic transformation in $A15$ compounds, Phys. Rev. B **14**, 1887 (1976).

[81] W. L. McMillan, Microscopic model of charge-density waves in $2H$-$TaSe_2$, Phys. Rev. B **16**, 643 (1977).

[82] U. Chatterjee, J. Zhao, M. Iavarone, R. Di Capua, J. P. Castellan, G. Karapetrov, C. D. Malliakas, M. G. Kanatzidis, H. Claus, J. P. C. Ruff, F. Weber, J. van Wezel, J. C. Campuzano, R. Osborn, M. Randeria, N. Trivedi, M. R. Norman, and S. Rosenkranz, Emergence of coherence in the charge-density wave state of $2H-NbSe_2$, Nat. Commun. **6**, 6313 (2015).

[83] K. Cho, M. Kończykowski, S. Teknowijoyo, M. A. Tanatar, J. Guss, P. B. Gartin, J. M. Wilde, A. Kreyssig, R. J. McQueeney, A. I. Goldman, V. Mishra, P. J. Hirschfeld, and R. Prozorov, Using controlled disorder to probe the interplay between charge order and superconductivity in $NbSe_2$, Nat. Commun. **9**, 2796 (2018).

[84] L. Li, X. Deng, Z. Wang, Y. Liu, M. Abeykoon, E. Dooryhee, A. Tomic, Y. Huang, J. B. Warren, E. S. Bozin, S. J. L. Billinge, Y. Sun, Y. Zhu, G. Kotliar, and C. Petrovic, Superconducting order from disorder in $2H-TaSe_{2-x}S_x$, npj Quantum Mater. **2**, 11 (2017).

[85] H. Mutka, Superconductivity in irradiated charge-density-wave compounds $2H$-$NbSe_2$, $2H$-TaS_2, and $2H$-$TaSe_2$, Phys. Rev. B **28**, 2855 (1983).

[86] M. Leroux, V. Mishra, J. P. C. Ruff, H. Claus, M. P. Smylie, C. Opagiste, P. Rodière, A. Kayani, G. D. Gu, J. M. Tranquada, W.-K. Kwok, Z. Islam, and U. Welp, Disorder raises the critical temperature of a cuprate superconductor, Proc. Natl. Acad. Sci. USA **116**, 10691 (2019).

[87] T. Moriya and K. Ueda, Spin fluctuations and high temperature superconductivity, Adv. Phys. **49**, 555 (2000).

[88] P. A. Lee, N. Nagaosa, and X.-G. Wen, Doping a Mott insulator: Physics of high-temperature superconductivity, Rev. Mod. Phys. **78**, 17 (2006).